ELSEVIER

European Journal of Pharmaceutics and Biopharmaceutics 46 (1998) 243–254

European Journal of Pharmaceutics and Biopharmaceutics

Research paper

Chemo-embolization of experimental liver metastases. Part I: distribution of biodegradable microspheres of different sizes in an animal model for the locoregional therapy

P. Bastian[a], R. Bartkowski[b], H. Köhler[b], T. Kissel[a,*]

[a]*Department of Pharmaceutics and Biopharmacy, Philipps-University, Marburg, Germany*
[b]*Department of General Surgery, Georg-August-University, Göttingen, Germany*

Received 24 March 1997; accepted 22 April 1998

Abstract

An experimental in vivo rat model was established to simulate the embolization therapy of non-resectable liver metastases with microparticulate systems. The effects of biodegradable microspheres on a transplanted liver-tumor cell line in rat livers were investigated with respect to particle size. The distribution of fluorescence-labelled microspheres was investigated to characterize the effects of long-term embolization with biodegradable microspheres, and the suitability and relevance of this animal model. Novikoff hepatoma cells were implanted into the central liver lobe of Sprague–Dawley rats. After seven days, four batches of fluorescence-marked microspheres (17 μm, 25 μm, 30 μm, and 40 μm) were administered into the proper hepatic artery. Liver(including the tumor), lung and spleen were isolated and frozen sections and tissue cubes of liver-, border-, and tumor tissue were prepared. The sections were examined by fluorescence microscopy. The cubes were extracted and the fluorescence of the marker quantified. During operation, microspheres smaller than 40 μm did not cause complete embolization. The slides showed the spreading of the smaller particles to the spleen and lung. Only 40 μm particles accumulated in the liver and were rarely detectable in other organs. The extraction showed a high concentration of the 40 μm particles in the border tissue. Apparently they were trapped proximal to the tumor capillary system and therefore showed a high ratio of border/tumor concentration. Microparticles smaller than 40 μm had a border/tumor concentration ratio of less than one and were distributed to the spleen and lung. In conclusion, a mean particle diameter of at least 40 μm is required for embolization. Thus, the model shows similarity to clinical situations in the treatment of human liver tumor and metastases.

Keywords: Microparticles; Poly(D,L-lactide-co-glycolide); Embolization; Chemo-embolization; Liver metastases; Hepatoma

1. Introduction

Both types of neoplastic malignancies of the liver, hepatocellular carcinoma and hepatic metastases, are still a challenge for chemotherapy.

Hepatocellular carcinoma is, worldwide, the third most common form of cancer with a geographical prevalence in Southeast Asia and southern Africa [1,2].

Patients show a median survival of 4 months from the date of diagnosis [3], and the most successful therapy by surgical resection is only possible in 30% of all cases [4]. Still, there remains a high recurrency rate with a limited survival rate [5,6].

Liver metastases are not restricted to certain geographic areas, in 80% of all cases they are derived from colorectal carcinomas and further from malignancies of the stomach, the pancreas, and other cancer types [3]. In 30–50% of all patients dying from malignant tumors, hepatic metastases in

* Corresponding author. Department of Pharmaceutics and Biopharmacy, Ketzerbach 63, D-35037 Marburg, Germany. Tel.: +49 6421 285881; fax: +49 6421 287016; e-mail: kissel@mailer.uni-marburg.de

0939-6411/98/$19.00
PII S0939-6411(98)00047-2

the liver are detected [3]. Surgical resection can only be performed in less than 10% of the cases due to histological limitations [3].

Several therapy regimens have been proposed. General cytostatic or radiologic therapies have proven to be of limited success especially because of the serious side effects [7,8]. Therefore, it has become general practice to exploit regional therapeutic advantage. Hepatic arterial infusion of chemotherapeutic agents was advantageous over systemic chemotherapy [9,10] but the effect on survival is still poor. Different devices have been invented to enhance the regional advantage by blood flow reduction [8]. Ligation with mechanical devices [11,12] had the disadvantage of causing severe side effects like hepatic necrosis, hepatitis, or hepatic failure [13]. Injected or implanted blocking materials, such as silicone rubber, gelatin sponge, or balloon catheters [8,12], had similar side effects.

The therapeutic tendency today shifts towards a regional enhancement of drug concentration and exposure-duration by reduction of the arterial blood flow by lipiodol [14,15] or microspheres such as degradable starch microspheres [16–18]. This concept is based on a transient effect of blood flow reduction and, therefore, often requires multiple dosing to achieve a significant advantage in therapy [19].

A combination of the long-term embolization with an enhanced regional drug concentration could be achieved with drug loaded poly(D,L-lactide-co-glycolide) microspheres, injected into the hepatic artery. Their release properties and degradation times can be adjusted by variation of the polymer composition. For example, a release of a cytostatic agent over a period of about 4 weeks can be achieved before the microparticles degrade to non-toxic products.

The goal was to perform an animal study with poly(D,L-lactide-co-glycolide) microspheres to simulate embolization therapy and define the optimum particle size and dosage as well as to detect the microparticle distribution by the blood stream and the location site.

2. Materials and methods

2.1. Materials

Poly(D,L-lactide-co-glycolide) 50:50 (RG 503) was obtained from Boehringer Ingelheim (Ingelheim, Germany) and fluoresceine dilaurate (FDL) was purchased from Sigma Chemical (St. Louis, MO, USA). Degradable starch microspheres (Spherex®) were obtained from Pharmacia, Freiburg. All other chemicals were of analytical grade.

Table 1

Microparticle preparation: variation of the parameters

Batch	Ratio CH_2Cl_2:aqu. (v/v)	Ratio RG503:CH_2Cl_2 (m/V)	d_v 0.5 (±SD, μm)	cFDL (%m/m)
MP40	1:10	1.3:10	40.2 ± 0.54	0.368
MP30	1.5:10	1:10	29.5 ± 0.56	0.709
MP25	1:10	1:10	25.4 ± 0.10	0.296
MP17	2.5:10	0.75:10	17.8 ± 0.02	0.386
DSM	–	–	45	–

Table 2

Microscopic evaluation of the particle size distribution

Rat no.	Size of MP (μm)	Tumor	Liver	Spleen	Lung
1	40	+	++	+	+
2	40	+	+++	–	–
9	40	(+)	+++	(+)	+
5	30	++	++	++	+++
8	30	+	++	+	+
4	25	++	+	++	+++
6	25	++	+	+	++
3	17	+++	++	+++	+++
7	17	++	++	+	+++

–, No MP were found in all slices; (+), rarely detected single microparticles or small agglomerates with less than 10 MP in all slides; +, less than 10 agglomerates and about 10 single MP in all slides; ++, between 10 and 30 agglomerates and up to 150 MP per slide; +++, more than 30 agglomerates and uncountable single MP per slide.

2.2. Microparticle preparation

Microparticles (MP) were prepared by a modified solvent evaporation method [20]). Briefly, FDL and RG 503 were dissolved in methylene chloride and this organic phase was emulsified in 0.5% aqueous PVA-solution (Mowiol 18–88, Hoechst AG, Frankfurt, Germany; 87.7% hydrolysed) by stirring at a rate of 2200 rev./min for 3 h with a four-blade propeller stirrer (Heidolph Elektro KG, Kelheim, Germany). Afterwards, the particles were collected by centrifugation, washed twice with water and dried under vacuum for 24 h. Different particle sizes were adjusted by variation of the volume ratios of external and internal phase and the viscosity of the organic phase. Table 1 shows the different compositions. Four batches with the following particle sizes (d_v 0.5) were prepared: 40 μm (MP40), 30 μm (MP30), 25 μm (MP25), and 17 μm (MP17). Particle sizes were determined in an aqueous 0.02% Tween 80 solution in a Master-Sizer X (Malvern Instruments, UK). The differences between the batches were shown by subtraction of the volume distributions and the mean values of the volume distribution (d_v 0.5), the weighted means (D 4.3), the span (s) and the volume fraction of small particles were evaluated (Table 2). The formulas for these characteristic numbers are given in Eqs. (1) and (2).

$$D[4,3] = \frac{\sum nd^4}{\sum nd^3} \quad (1)$$

$$s = \frac{s_v 0.9 - d_v 0.1}{d_v 0.5} \quad (2)$$

where n is the number of particles per fraction; d, mean

diameter of each fraction; d_v (0.1), limiting diameter of 10% of the particle volume in μm; d_v (0.9), limiting diameter of 90% of the particle volume in μm.

The particles were of spherical shape and had a relatively smooth surface as demonstrated in the SEM photos (Fig. 2) taken by a scanning electron microscope (Hitachi S510, Nissei Sangyo GmbH, Dusseldorf, Germany).

2.3. Animals

Nine female Sprague–Dawley rats (Fa. Dinkelmann, Paderborn) (bodyweight 200 ± 20 g) were housed in a temperature- and humidity-controlled room with free access to water and standard rat feed. The principles of laboratory animal care and the German animal protection laws (1993) were strictly followed.

2.4. Tumor model

Novikoff hepatoma cells (5×10^5) were injected under the capsule of the central liver lobe [21] in female Sprague–Dawley rats to induce single tumor nodules. As investigated in laparoscopies, the tumors had to be larger than 4 mm^3 to be acceptable for further investigations and the ratio of failure was less than 5%. Seven days after tumor inoculation the tumors were suitable for embolization, whereas older tumors were too large and showed spontaneous necrosis. Under ether anesthesia a laparotomy was performed.

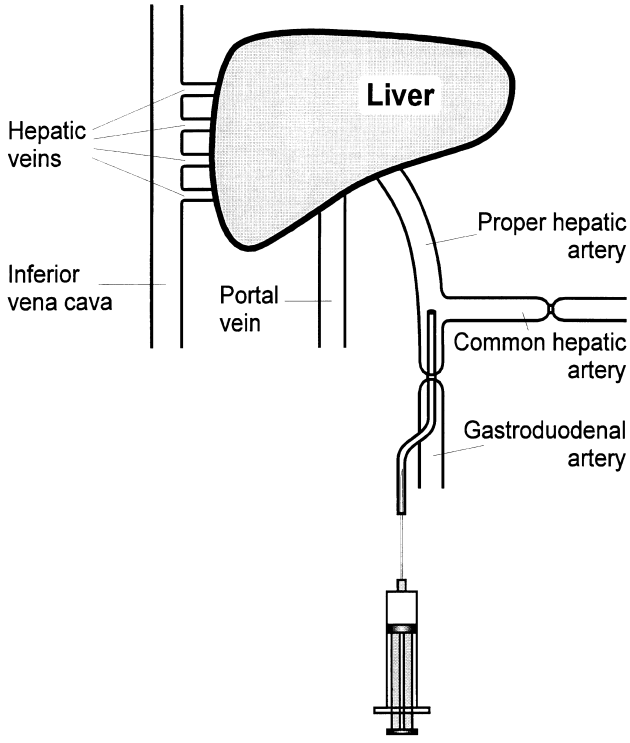

Fig. 1. Scheme of the application technique. A polyethylene catheter was introduced, with its tip placed at the junction of the common hepatic artery. This artery had been clamped during the application to prevent backflow of the microparticles.

During observation with an operating microscope the gastroduodenal artery was cannulated using a polyethylene catheter (Portex PP10). The tip of the catheter was placed at the origin of the proper hepatic artery. The MP were suspended in 0.1% isotonic Pluronic F68-solution in a concentration of 30 mg/ml and injected through a syringe and a needle into the catheter. During the application of the suspension over a period of 5 min the common hepatic artery was clamped to prevent retrograde flux (Fig. 1) and the embolization was controlled by the operating microscope. Animals 1, 2, and 9 received MP40 and a complete embolization was achieved. The injection was aborted when the MP accumulated in the tip of the catheter so that a total amount of 50 mg MP was applied to animals 2 and 9 and 90 mg were applied to animal 1. All of the smaller amounts of MP did not cause total embolization so that the injection was stopped after application of 100 mg MP.

2.5. Tumor measurement

According to the literature [22] the tumor size was evaluated by the following method:

$$S = 0.5 \times D1 \times D2^2$$

where S is the tumor size (mm^3), $D1$ is the largest diameter (mm) and $D2$ is the smallest diameter (mm) of the tumor.

2.6. Tissue preparation

Five minutes after the treatment the animals were euthanized. The artery was clamped, the liver was prepared and the connective tissue was dissected. The liver was removed and trimmed to a block of liver tissue and medial tumor tissue. The tumor and the liver tissue were dissected in the lateral tissue and all tissue parts were wrapped in aluminium foil and frozen in liquid nitrogen. The frozen block was cut into cubes of about $2 \times 2 \times 2$ mm^3 and the tissue from the liver and the tumor was identified. Cubes which contained both tumor and liver tissue were described as border tissue.

One lateral part with evident median tumor tissue was used to prepare frozen sections of 20 or 30 μm thickness in a freeze microtome Frigocut 2800 (Leica, Hamburg, Germany).

Furthermore, the lung and the spleen were prepared and removed from the animals and frozen sections were obtained in the same way.

2.7. Microscopic analysis

The frozen sections were screened under a Zeiss light microscope equipped with fluorescence filters and a phase contrast optic long pass filter system (Zeissbarrier LP520 nm dichroic mirror FT510 nm exciter 450–490 nm). The density of the particles in the organs was evaluated by counting. All slides were investigated and a classification was obtained as described in Table 2.

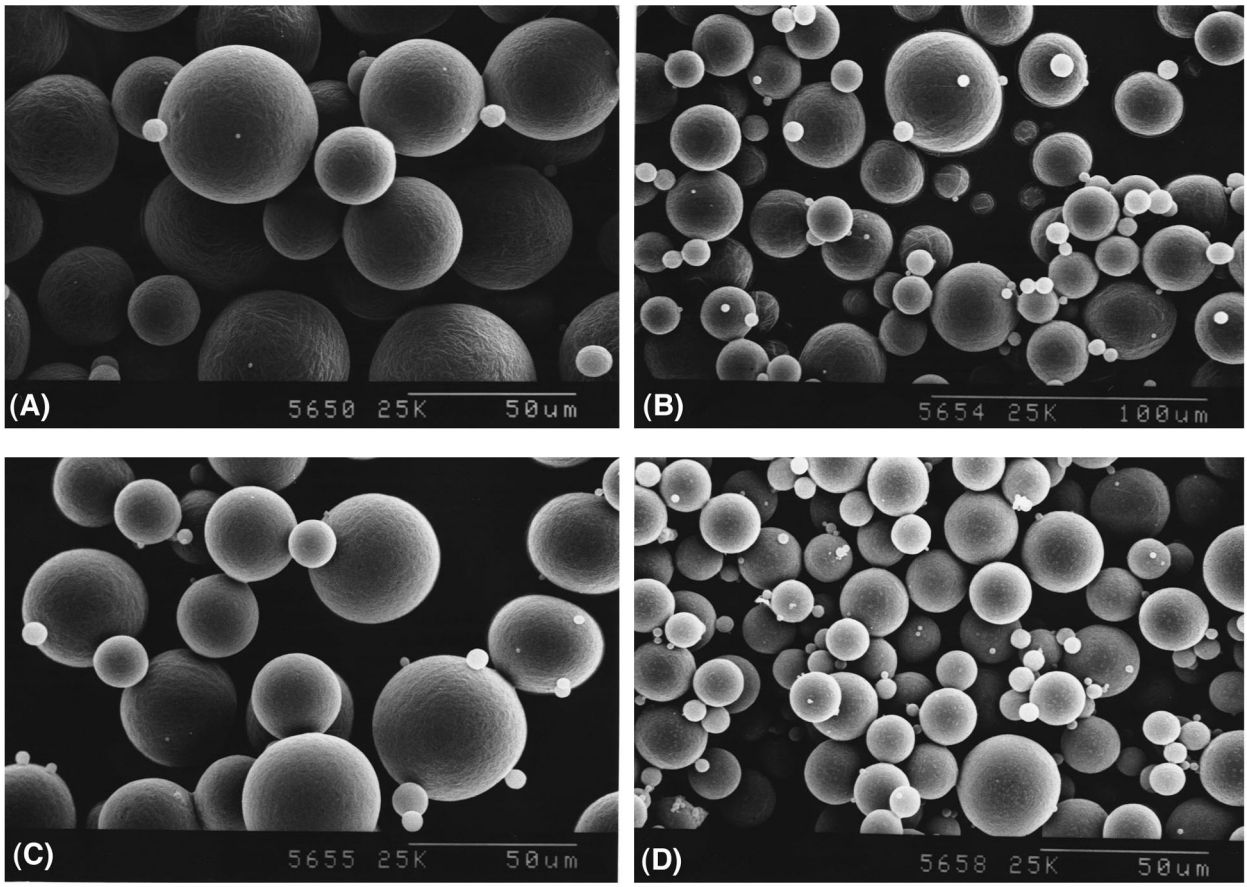

Fig. 2. SEM micrography of the MP. (A) MP40; (B) MP30; (C) MP25; (D) MP17.

2.8. Analysis of FDL-containing particles in the tissue

Each cube of the liver-, border-, and tumor-tissue was homogenized in 10 ml distilled water and extracted twice with 10 ml methylenechloride. The lipophilic FDL in the organic phase was hydrolyzed by 1.5 ml 10% methanolic potassium-hydroxide solution and, after 5 min, the fluoresceine was extracted twice by 5 ml aqueous phosphate buffer (pH 7.4). The aqueous solution was collected and diluted with phosphate buffer (pH 7.4). Both extraction steps were standardized. A calibration curve for fluoresceine was measured with a correlation coefficient of 0.99886. The hydrolysis of FDL in methylene chloride and extraction by aqueous buffer was standardized with a correlation coefficient of 0.9957, and the determined vs. the expected value showed a coefficient of 0.9999. Standards were analysed together with the extraction of the samples, and a liver blank was determined. The fluorescence was measured in a Fluorispec SF-100 fluorescence spectrophotometer (Baird-Atomic Europe N.V.). The content of FDL in the MP was also determined after dissolving them in 20 ml methylene chloride, hydrolyzing with 1.5 ml 10% methanolic potassium-hydroxide solution and double extraction with 5 ml aqueous phosphate buffer. The values are also given in Table 1.

3. Results

3.1. Microparticle preparation and characterisation

Four batches of microspheres (MP) were prepared by the solvent evaporation method [23]. The different particle size distributions were achieved by variation of the preparation parameters (Table 1). Reduction of the volume of the internal organic phase and reduction of the viscosity of the internal phase by using a lower RG 503 concentration led to larger particles.

The MP had a mean volume diameter (d_v) of 40 μm (MP40), 30 μm (MP30), 25 μm (MP25), and 17.8 μm (MP17). Their particle size distributions were measured with a mastersizer and are shown in Fig. 3. All batches contained a volume part less than 10% of particles smaller than 10 μm (Table 2) except MP17, which showed a fraction of 11.67% less than 7.01 μm. The maxima of the batches contained 30% of the volume of the particles.

The differences in particle size distribution of the batches were obtained by subtraction (Fig. 5). The larger the values, the better is the discrimination between the different batches. The absolute values depend on the maxima of each particle size distribution. The graphs show the relative quantity that both batches do not have in common.

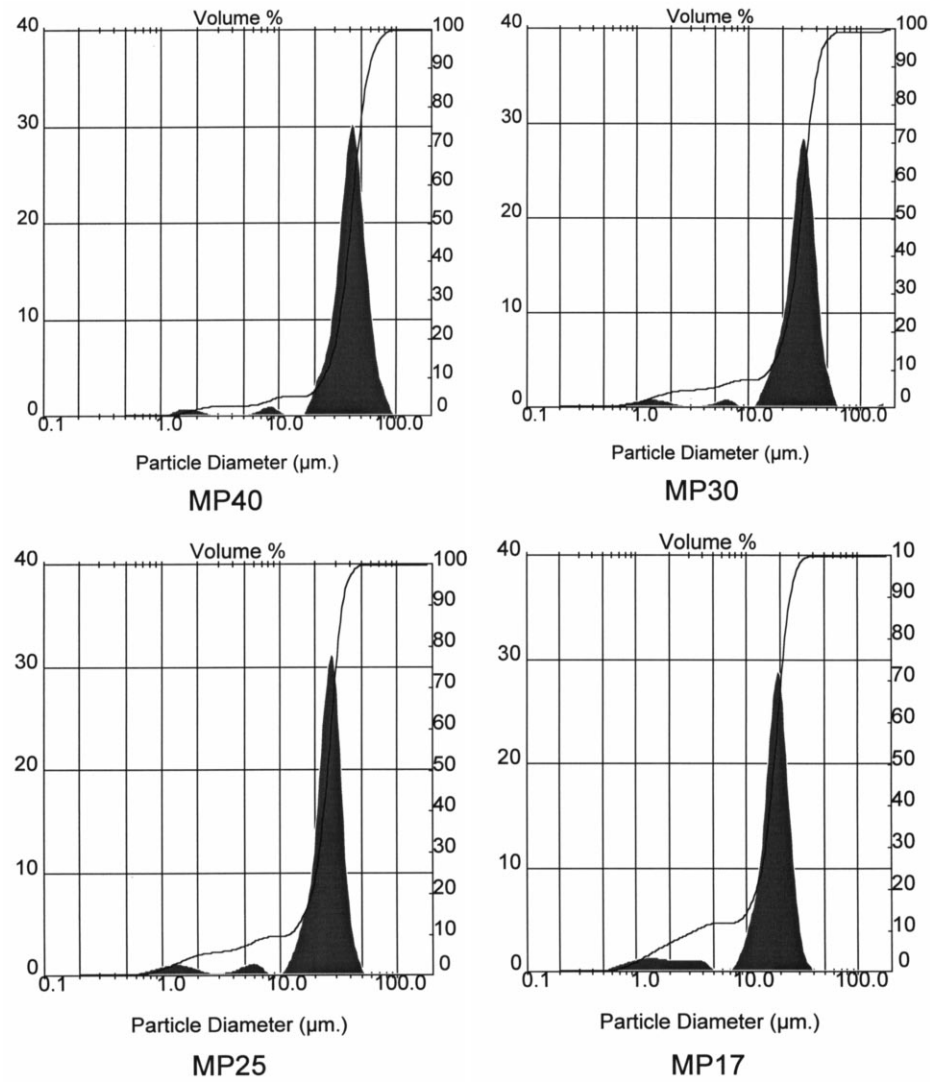

Fig. 3. Particle size distributions of the four MP batches.

In Table 1 the median diameter of the volume of the particles (d_v 0.5), the weighed diameter of the distributions (D (4.3)) and the spans (s) of the distributions are given. The differences between d_v 0.5 and D (4.3) are not significant, which can be interpreted as a sign of the low agglomeration tendencies of the particles.

It can be seen from the subtraction of the distributions that MP17 and MP25 as well as MP30 and MP40 can be distinguished.

The SEM pictures (Fig. 2) show round and discrete MP with a relatively smooth surface in all batches.

3.2. Comparison with DSM

The size distribution of clinically used degradable starch microspheres (DSM, Spherex®, Pharmacia) is similar to MP40 (Fig. 4). Less than 10% of the volume is smaller than 10 μm and the distribution shows a d_v (0.5) of 45 μm.

As differences of the subtracted distribution functions are low, a good similarity between MP40 and degradable starch microspheres is observed. The d_v (0.5) is 4.25 μm larger than that of MP40 but, as the higher difference between d_v (0.5) and D (4.3) shows, the tendency of agglomeration is slightly higher in degradable starch microspheres than in MP40.

The volume fraction of the particles less than 10 μm in diameter is nearly 2% higher than in MP40 (Table 2).

3.3. Animal model

The implantation of the tumors by a single injection of tumor cells turned out to be uncomplicated. Nine of ten rats showed tumors after seven days, which fulfilled the principle prerequisite to be larger than 4 mm^3 in size.

A microsurgical procedure analogous to [24] was performed as demonstrated in Fig. 1. The size of the gastroduodenal artery was limiting the catheter size (Portex PP10)

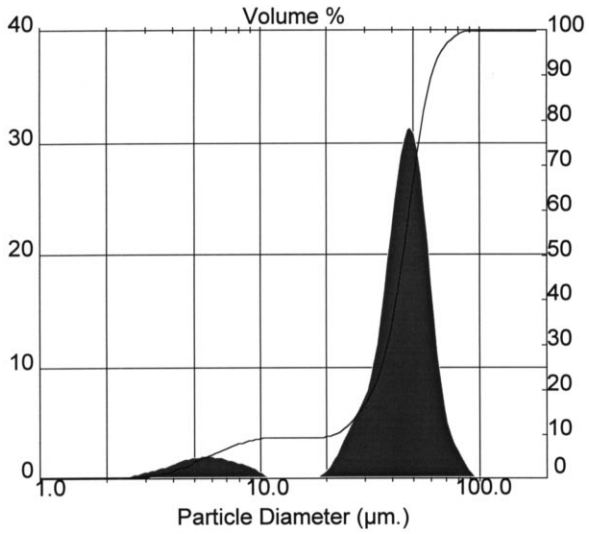

Fig. 4. Particle size distribution of DSM (Spherex).

and was consequently controlled the largest particle size of 40 μm.

The investigation of the microsurgical procedure and the application of the MP in nine animals by an operating microscope led to a primary observation: the 40 μm MP caused total embolization in all three animals with complete filling of the artery up to the tip of the catheter. The applicable amount of MP, therefore, was limited to 50, 90 and 100 mg.

The smaller MP did not show full embolization, so that the injection was aborted after 100 mg.

3.4. Microscopic evaluation

The examination of the frozen sections of tumor-, liver-, spleen, and lung-tissue using a fluorescence microscope showed single MP, as well as agglomerations in all slides, similar to previous observations in the literature [25] (Fig. 6).

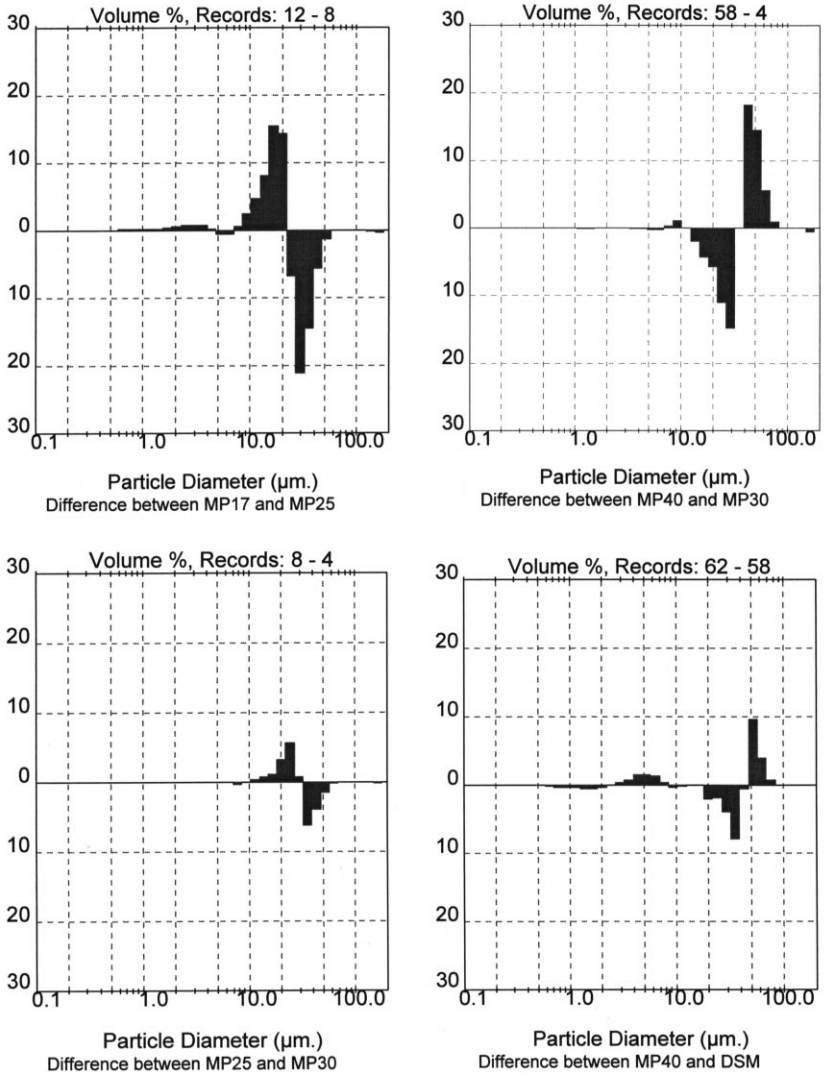

Fig. 5. Differences of the functions of the particle distributions obtained by subtraction.

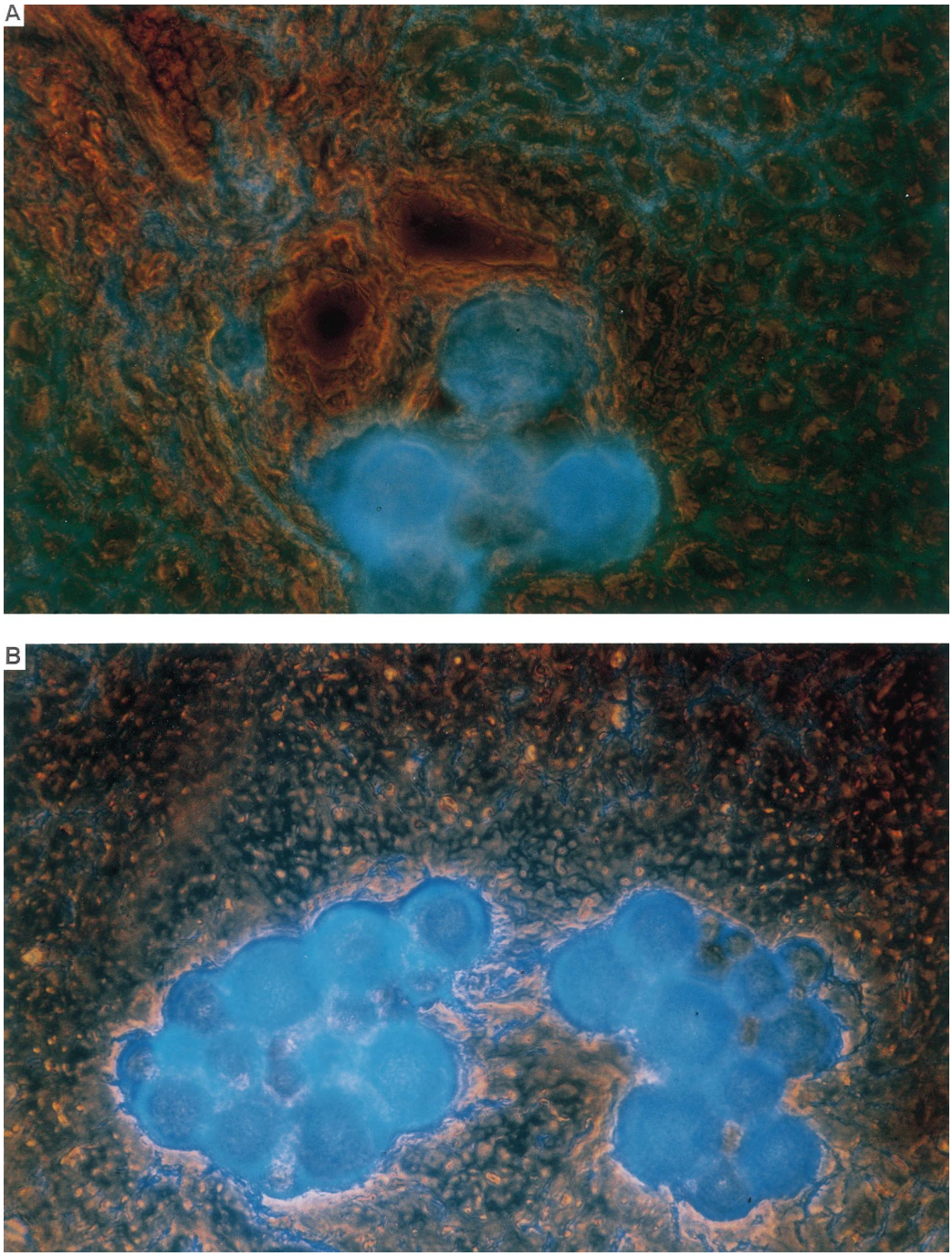

Fig. 6. Micrography of fluorescence-labelled MP agglomerates in vessels.

As clearly visible in liver tissue, the MP are located in vessels and occlude them completely (Fig. 7).

All slides were examined and the total number of MP or agglomerates per tissue type was semiquantitatively evaluated (Table 3).

Mainly particles smaller than 40 μm were detected in the tumor tissue, (more than 10 agglomerates and single MP). MP17 had the highest density (more than 30 agglomerates per slice and uncountable single MP) whereas only less than 10 agglomerates and about 10 single MP of MP40 were present.

In contrast, a high number of MP40 (more than 10 agglomerates and many single MP) were detected in the liver tissue.

MP smaller than 40 μm were present in a high concentration (more than 10 agglomerates and single MP) in the spleen and lung. Subsequent sections showed that the smaller particles were distributed in remote parts of the lung

especially as single particles, whereas larger particles agglomerated in the main branches of the vessels. MP40 were rarely detected in spleen or lung.

3.5. Extraction studies

For isolation and dissolution of the poly(D,L-lactide-co-glycolide)-microspheres, the tissue cubes were dispersed in water and extracted with methylenechloride. The lipophilic FDL accumulated in the organic phase. It was hydrolyzed to Fluoresceine by methanolic potassium hydroxide solution, extracted with water, neutralized and diluted in aqueous phosphate buffer (pH 7.4). The concentration was measured by fluorescence spectroscopy.

Fluoresceine standards showed a linearity with a regression coefficient of 0.9989. The extraction steps were controlled by standards and a linearity between the obtained values and the original concentration was obtained. The calculation of the concentration was based on standards.

Fig. 7. Micrographies of MP in vessels of liver tissue.

Table 3

Characteristic values of the particle size distributions

	d_v 0.5 (μm)	D 4,3 (μm)	Limit of the small fraction (μm)	s
DSM	44.19	42.07	9.28% < 10.27	0.81
MP40	39.94	38.89	7.28% < 10.27	0.82
MP30	29.10	29.36	7.25% < 10.00	0.89
MP25	25.29	24.02	9.68% < 10.27	0.89
MP17	17.78	17.00	11.67% < 7.01	1.24

The highest absolute tissue concentration, in total. was found at an application of MP40 (Fig. 8D).

The highest concentration in the tumor tissue was obtained with MP17.

There were no characteristic patterns of the MP concentrations in the liver tissue (data not shown).

In the border tissue between normal liver and tumor tissue, a high concentration of MP40 was found whereas all other MP were less concentrated there. This was even evident when the border tissue was added to the tumor tissue in the calculation (T + B) (Fig. 8B).

The comparison between border tissue and tumor tissue (Fig. 9) highlights the higher concentration of MP40 in the border tissue than in the tumor tissue. MP30 levels are sometimes higher and sometimes lower in the border than in the tumor tissue. Smaller particles were less concentrated in the border tissue than in the tumor. This is also expressed by the ratio of the concentration in the border tissue versus the concentration in the tumor tissue (Fig. 10). The ratio of MP40 is much higher than 1, the ratio of MP30 about 1 and the ratio of smaller particles is less than 1.

4. Discussion

4.1. Microparticle preparation and characterisation

As previously described in clinical application and in animal experiments [31,32], 40 μm particles caused the most distal embolization with the least induction of collaterals. For comparison reasons particles of 40 μm in diameter or smaller were of interest.

The SEM demonstrated (Fig. 2) discrete and spherical particles with a relatively smooth surface, which were easily suspended for application in a 0.1% Pluronic F68 solution, using ultrasound. During the injection, the solution was shaken in the syringe several times to prevent sedimentation.

Due to the preparation of the microparticles in a solvent evaporation process, the particle size distribution showed a fraction of particles smaller than 10 μm in all batches (Fig. 3). The volume part of this fraction was less than 10% in

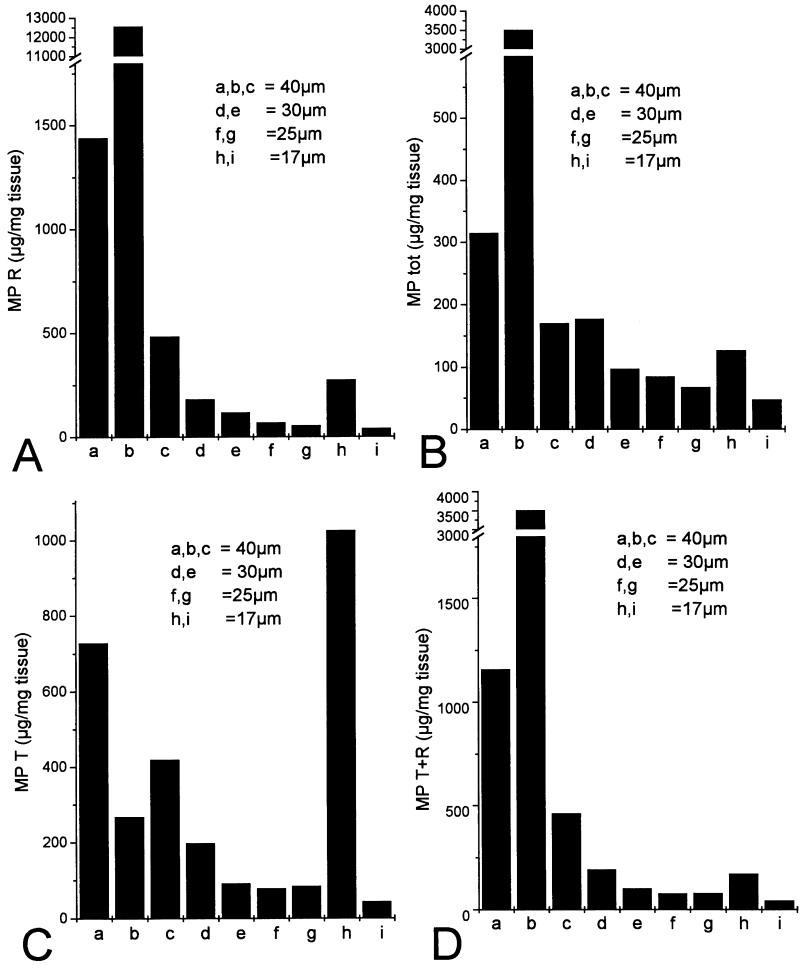

Fig. 8. Concentration of MP in different tissue types: (A) Border tissue (R) (B) Tumor + border (R) tissue (C) Tumor tissue; (D) In the whole sample of each animal.

most batches and DSM showed the same distribution characteristics (Figs. 4 and 5). DSM is already established in clinical use [19]. No severe side effects have been associated with this part of the MP batches yet.

The MP40 show nearly identical values in span as DSM. They show slightly better characteristics in the volume fraction of particles less than 10 μm and a better agreement of the d_v 0.5 with the D (4.3) (Table 2).

As visible in the micrography (Fig. 7), MP40 caused a complete embolization with totally filled vessels. In the microscopic counting, few microparticles were detected in two cases and no microparticles in one case. This leads to the suggestion that the small microspheres cannot pass the vessel system after complete embolization and therefore are also retained in the liver. The passage of the few observed particles could not be connected with any kind of pulmonary side effect in the animals.

MP40 and MP30 as well as MP25 and MP17 differed by more than 20% (volume) in their maxima. The maxima themselves were about 30%. The similarity between these batches was much greater than between MP30 and MP25 which differed less than 10% (Fig. 5).

4.2. Comparison to DSM

DSM showed agglomerated and deformed structure on the SEM micrographs. Their ability to swell and to be deformed has been previously described in the literature as the ability to fit in the arteries under slight pressure [26]. Nevertheless, they had a smooth surface.

The size distribution looks rather similar to our batches with 10% MP smaller than 10 μm (Table 3).

The DSM had a d_v (0.5) of 45 μm in accordance with the literature [26] and seemed slightly larger than MP40, but, the difference in the particle size distributions of MP40 and DSM was less than 10% (volume) in each fraction, so that they were comparable in this respect (Fig. 5).

The main difference between DSM and the prepared microspheres is the degradation time of the MP. DSM degrades within about 25 min [26] and therefore leads to a transient reduction of arterial blood flow. Its therapeutical benefit is gained through an enhancement of the co-administrated drug effect during this short treatment period [33–35].

In contrast, MP degrade within 30–50 days and are,

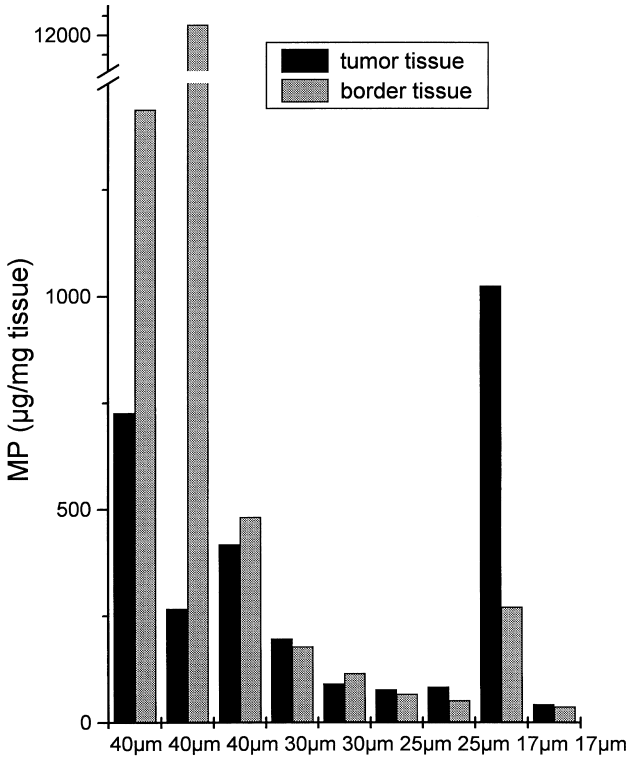

Fig. 9. MP concentration (μg/mg tissue) in the border and tumor tissue.

therefore, intrinsically more stable than DSM, leading to a long-term embolization combined with a release of cytostatic agents.

4.3. Microscopic evaluation

As seen in the slides (Table 2), all MP appeared in the tumor as well as in the liver tissue. They were distributed as single particles or agglomerated in the vessels as more-or-less large masses (Figs. 6 and 7). The size of the agglomerations was a few particles up to about 60 MP per accumulation.

The counting of the MP was difficult because of the various distributions of blood vessels. Parts existed with lots of MP whereas other parts did not show any [25]. All slides were evaluated in total to ensure that the counts were representative for the organ distribution.

The ranking of the evaluation (Table 3) rates the detection of a small amount (less than 10 single or agglomerated MP) of MP higher than a large amount (more than 30 agglomerates and uncountable single MP per slide) and this conforms with the aim to discriminate between total or no embolizing effect.

The high concentration of MP17 in tumor tissue could, by mistake, lead to the conclusion that the smallest MP achieve the best targeting effect. But it was observed, even during the application, that MP17 did not cause embolization. All batches smaller than 40 μm were well distributed to the spleen and lung. Only MP40 were almost undetectable in lung and spleen and were predominant in the liver tissue.

This means that MP40 were mainly trapped in the liver tissue. They entered the tumor only in low concentrations, and were rarely washed out into the organism.

4.4. Extraction studies

Three classes of cubes were obtained: tumor tissue, liver tissue, and cubes that contained both, called ‘border tissue’. This region is of special importance for tumor growth and vascularization.

A high total concentration of MP40 seemed to be due to complete embolization without wash-out effect (Fig. 8d). Nevertheless MP40 were detected in the tumor tissue (Fig. 8c).

One animal with MP17 showed a high tumor concentration analogous to the microscopical findings.

The high concentration of MP40 in the border tissue (Figs. 8 and 9) shows that the particles were mainly transported to the border of the tumor where they were trapped in the region of the capillaries.

Fig. 10 shows a summary of the ratio of border/tumor tissue and the location of the MP.

MP40 showed a very high ratio which means that they are in a higher concentration in the border tissue than in the neighbouring tumor tissue. MP30 show a ratio of about 1, they are distributed to the tumor in the same manner as to the border tissue. All other tissues show a ratio lower than 1. They were not retained in the border tissue and transported to the tumor.

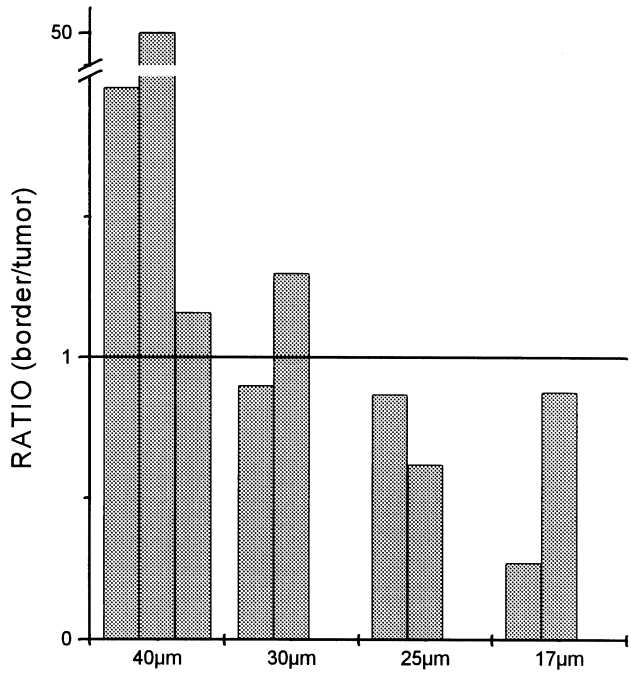

Fig. 10. Ratio of border (B) versus tumor (T) tissue in dependency of particle size.

4.5. Comparison of the results

The observation at the application, that only MP40 caused a full embolization, is congruent with the result from the microscopical examination, that smaller MP than 40 μm are washed out from the liver and transported to other organs. The extraction study confirmed these findings and showed that the MP were mainly trapped directly in front of the tumor. This ensures a complete embolization with temporary arrest of the blood flow, and all intended further harm, to the tumor.

Even if the main part of the applied MP is not directly located in the tumor itself, the distance to tumor tissue is small and any incorporated drug could easily diffuse to the tumor cells. This also leads to an enhanced drug concentration.

The aspect of complete embolization seems to be more important than the direct location of MP in the tumor tissue. Without total embolization, the concentration of the MP would be reduced by a washout and the risk of severe side effects especially in the lung would arise.

The well-known clinical necessity for individual dosing [27] is also shown here. At total embolization, the vessel system was filled with an individually differing amount of MP. Thus, the injection had to be stopped once after the application of 50 mg and twice after 90 mg.

Similar results were obtained in white New Zealand rabbits that had had implanted VX2 tumors [25] using polystyrene MP. The microscopic examination showed both clustered and individually distributed MP. The tumor concentration of the 27 μm MP was also higher than in the liver, but there was no control of complete embolization. As in our case, the only way of selective tumor targeting seems to be the trapping of the large MP proximal to the smaller tumor capillary system at the border between liver and carcinomatous tissue.

In a further study the distribution of ^{125}I labelled albumin-MP of 12.5 μm, 25 μm, and 40 μm diameter was studied in rats bearing HSN sarcoma in the liver [28]. The administration of the MP was similar to this study. However, the results did not show any clear differentiation in the detection of the various MP batches and a full embolization was not observed.

The HSN sarcoma model took 20 days to develop reproducible tumors, whereas the Novikoff hepatoma was suitable for embolization after 7 days. The Novikoff hepatoma model has proved to be appropriate for chemotherapy studies. It is derived from the epithelial tissue and is highly resistant to systemic chemotherapy, so that it seems to be quite similar to the clinical situation.

Smaller fluoresceine-loaded MP (2–5 μm) were used to detect their distribution to various organs after venous application in mice [29], therefore, frozen sections were also screened under fluorescence microscopy.

A distribution to lung and liver in mice [30] was also detected with smaller MP of polylactide less than 10 μm diameter. Even in mice, smaller particles were not suitable for embolization and the different principle of targeting was less successful than ours.

Once the embolization is complete, not even smaller particles will be transported in the filled vessel system, so that only a small part of the less than 10 μm large MP could be transported in the body circulation at the beginning of the application. Therefore, the part of the smaller MP should not contribute to severe side effects.

Observed in many clinical studies, the MP of 40 μm in diameter are very useful for application in patients [19].

References

[1] D.M. Keehn, M. Frank-Stromborg, A worldwide perspective on the epidemiology and primary prevention of liver cancer, Cancer Nursing 14 (1991) 163–174.

[2] D. Parkin, J. Stjernsward, C. Muir, Estimates of the worldwide frequency of twelve major cancers, Bull. World Health Organization 62 (1984) 163–182.

[3] A. Moossa, S. Schimpff, M. Robinson, Comprehensive Textbook of Oncology, Williams and Wilkins, USA, 1991.

[4] D.G. Farmer, R.W. Busuttil, The role of multimodal therapy in the treatment of hepatocellular carcinoma, Cancer 73 (1994) 2669–2670.

[5] T. Harada, T. Shigemura, S. Kodama, T. Higuchi, S. Ikeda, M. Okazaki, Hepatic resection is not enough for large hepatocellular carcinoma, J. Clin. Gastroenterol. 143 (1992) 245–250.

[6] E.C. Lai, I.O. Ng, M.M. Ng, Long-term results of resection for large hepatocellular carcinoma: a multivariate analysis of clinicopathological features, J. Hepatol. 11 (1990) 815–818.

[7] N. Kemeny, Systemic chemotherapy of hepatic metastases, Semin. Oncol. 10 (1983) 148–158.

[8] W.D. Ensminger, J.W. Gyves, Regional cancer chemotherapy, Cancer Treatment Reports 68 (1984) 101–115.

[9] J.A. Goldberg, D.J. Kerr, D.G. Watson, N. Willmott, C.D. Bates, J.H. McKillop, C.S. McArdle, The pharmacokinetics of 5-fluorouracil administered by arterial infusion in advanced colorectal hepatic metastases, Br. J. Cancer 61 (1990) 913–915.

[10] D.J. Kerr, S.B. Kaye, Chemoembolism in cancer chemotherapy, Crit. Rev. Ther. Drug Carrier Systems 8 (1) (1991) 19–37.

[11] A.P. Hemingway, D.J. Allison, Complications of embolization: analysis of 410 procedures, Radiology 166 (3) (1988) 669–672.

[12] M.J. Pentecost, Transcatheter treatment of hepatic metastases, Am. J. Res. 160 (1993) 1171–1175.

[13] Y. Shibayama, Role of endotoxaemia in the development of hepatic failure following hepatic artery occlusion, J. Pathol. 161 (1990) 321–325.

[14] T. Ichida, M. Kato, A. Hayakawa, M. Watanabe, K. Igarashi, K. Hata, Y. Doya, M. Miura, H. Sato, H. Asakura, Treatment of hepatocellular carcinoma with a CDDP-epirubicin-lipiodol suspension: a pilot clinico-pharmacological study, Cancer Chemother. Pharmacol. 31 (Suppl.I) (1992) 51–54.

[15] J.L. Raoul, D. Heresbach, J.F. Bretagne, Chemoembolization of hepatocellular carcinomas. A study of the biodistribution and pharmacokinetics of doxorubicin, Cancer 70 (3) (1992) 585–590.

[16] K.F. Aronsen, C. Hellekant, J. Holmberg, U. Rothman, H. Teder, Controlled blocking of hepatic artery flow with enzymatically degradable microspheres combined with oncolytic drugs, Eur. Surg. Res. 11 (1979) 99–106.

[17] C. Fournier, M. Hamon, M. Hamon, J. Wannebroucq, S. Petiprez, J.-P. Pruvo, B. Hecquet, Preparation and preclinical evaluation of bioresorbable hydroxyethylstarch microspheres for transient arterial embolization, Int. J. Pharm. 106 (1994) 41–49.

[18] T.M. Hunt, A.D.S. Flowerdew, S.J. Birch, J.D. Williams, M.A. Mullee, I. Taylor, Prospective randomized controlled trial of hepatic arterial embolization or infusion chemotherapy with 5-fluorouracil and degradable starch microspheres for colorectal liver metastases, Br. J. Surg. 77 (1990) 779–782.
[19] T. Taguchi, N. Ogawa, B. Bunke, B. Nilsson, DSM Study Group (Japan), The use of degradable starch microspheres (Spherex) with intra-arterial chemotherapy for the treatment of primary and secondary liver tumours – results of a phase III clinical trial, Reg. Cancer Treat. 4 (1992) 161–165.
[20] N.B. Ackerman, W.M. Lien, E.S. Kondi, N.A. Silverman, The blood supply of experimental liver metastases. I. The distribution of hepatic arterial and portal vein blood to 'small' and 'large' tumors, Surgery 66 (1969) 1067.
[21] Y. Yamashita, M. Takahashi, Y. Koga, R. Saito, S. Nanakawa, Y. Hatanaka, N. Sato, K. Nakashima, J. Urata, K. Yoshizumi, K. Ito, S. Sumi, M. Kan, Prognostic factors in the treatment of hepatocellular carcinoma with transcatheter arterial embolization and arterial infusion, Cancer 67 (1991) 385–391.
[22] G. Carlsson, B. Gullberg, L. Hafström, Estimation of liver tumor volume using different formulas – an experimental study in rats, J. Cancer Res. Clin. Oncol. 105 (1983) 20–23.
[23] C. Grandfils, P. Flandroy, N. Nihant, S. Barbette, R. Jerome, Ph. Teyssie, A. Thibaut, Preparation of poly(D,L)lactide microspheres by emulsion-solvent evaporation, and their clinical applications as a convenient embolic material, J. Biomed. Mat. Res. 26 (1992) 467–479.
[24] R. Bartkowski, M.R. Berger, J.L.A. Aguiar, Experiments on the efficacy and toxicity of locoregional chemotherapy of liver tumors with 5-fluoro-2-deoxyuridine (FUDR) and 5-fluorouracil (5-FU) in an animal model, J. Cancer Res. Clin. Oncol. 111 (1986) 42–46.
[25] K.M. Pillai, P.E. McKeever, C.A. Knutsen, P.A. Terrio, D.M. Prieskorn, W.D. Ensminger, Microscopic analysis of arterial microsphere distribution in rabbit liver and hepatic VX2 tumor, Selective Cancer Ther. 7 (2) (1991) 39–48.
[26] H. Teder, N. Lundin, C.-J. Johansson, R. d'Argy, The effect of different doses of Spherex^{R} on the regional distribution of cytotoxic drugs in the rat, Reg. Cancer Treat. Suppl. 1 (1993) T8.
[27] S. Dakhil, W. Ensminger, K. Cho, J. Niederhuber, K. Doan, R. Wheeler, Improved regional selectivity of hepatic arterial BCNU with degradable microspheres, Cancer 50 (1982) 631–635.
[28] J.H. Anderson, W.J. Angerson, N. Willmott, D.J. Kerr, C.S. McArdle, T.G. Cooke, Regional delivery of microspheres to liver metastases: the effects of particle size and concentration on intrahepatic distribution, Br. J. Cancer 64 (1991) 1031–1034.
[29] K. Ciftci, H.S. Kas, A.A. Hincal, T.M. Ercan, O.G. Güven, S. Ruacan, In vitro and in vivo evaluation of PLAGA (50/50) microspheres containing 5-fluorouracil prepared by a solvent evaporation method, Int. J. Pharm. 131 (1996) 73–82.
[30] K. Ciftci, A.A. Hincal, H.S. Kas, M.T. Ercan, S. Ruacan, Microspheres of 5-fluorouracil using poly(D,L-lactic acid): in vitro release properties and distribution in mice after i.v. administration, Eur. J. Pharmacol. Sci. 1 (1994) 249–258.
[31] J.W. Gyves, W.D. Ensminger, D. VanHarken, J. Niederhuber, P. Stetson, S. Walker, Improved regional selectivity of hepatic arterial mitomycin by starch microspheres, Clin. Pharmacol. Ther. 34 (2) (1983) 259–265.
[32] L. Hashimoto, K. Ouchi, M. Suzuki, S. Matsuno, Energy metabolism changes and oxidative attack after hepatic arterial embolization and chemoembolization in thioacetamide-induced cirrhotic livers, Res. Exp. Med. 191 (1991) 91–98.
[33] D. Civalleri, M. Esposito, R.A. Fulco et al., Liver and tumor uptake and plasma pharmacokinetic of arterial cisplatin administered with and without starch microspheres in patients with liver metastases, Cancer 68 (5) (1991) 988–994.
[34] B. Lindell, K.-F. Aronsen, B. Nosslin, Studies in pharmacokinetics and tolerance of substances temporarily retained in the liver by microsphere embolization, Ann. Surg. 187 (1) (1978) 95–100.
[35] A.K. Thom, E.R. Sigurdson, M. Bitar et al., Regional hepatic arterial infusion of degradable starch microspheres increases fluorodeoxyuridine (FUdR) tumor uptake, Surgery 105 (3) (1989) 383–392.